SPECTRAL ANALYSIS OF STRATOCUMULUS REFLECTANCE

G.A. Titov

Pacific Northwest National Laboratory, USA
Institute of Atmospheric Optics,
Siberian Branch of the Russian Academy of Sciences, Tomsk
Received November 10, 1998
Accepted November 10, 1998

Influence of the geometric averaging effect on the spatial spectrum of reflected radiation in the inhomogeneous stratocumulus clouds is studied by means of numerical simulation. The explanation of the scale break in the spatial spectrum in terms of the radiation smoothing effect is critically examined.

1. INTRODUCTION

Analysis of Landsat cloud images has shown that the cloud-reflected (in directions close to the zenith) radiation fields are not scale-invariant over the full range of the observable scales from ~ 100 km to ~ 30–100 m (Refs. 1 and 2). For the scales larger than 200–500 m, the spatial spectrum of the radiation field follows approximately the power law with a slope close to that of the spatial spectrum of liquid water path (optical depth) of clouds. At smaller scales, the radiation field is a much smoother function than the optical depth field. Such a scale break suggests an existence of some characteristic scale which separates two distinguishable scaling regimes or physical processes, each governing radiation field fluctuations on the corresponding spatial scales.

Evidently, the large-scale fluctuations of the radiation field are determined by variations of liquid water path (optical depth) of clouds. As to the radiation field smoothing on small spatial scales, the physical[1] and statistical[2] hypotheses, as well as geometric averaging,[3] associated with finite field of view (FOVs) of real detectors, and radiative smoothing[4,5] supposedly caused by horizontal radiation fluxes were proposed to explain the existence of the scale break in the spectrum. It should be recognized that all these hypotheses and explanations seem to be not well grounded, and the physics of this phenomenon is poorly understood as yet.

This paper studies the geometric averaging effect and its impact on the spatial spectrum of reflected radiation from inhomogeneous stratocumulus clouds. It also critically examines the explanations of the scale break in terms of the radiative smoothing effect. The next section briefly describes the used fractal model of stratocumulus clouds and a method of solution of three-dimensional (3D) radiative transfer equation. Section 3 discusses the effect of geometric averaging on the spatial spectra of albedo and the reflectance (into different solid angles) of clouds. Section 4 includes critical analysis of a weakness and evident shortcomings of the explanation of the scale break based on the radiative smoothing. The concluding section summarizes the main results obtained.

2. FRACTAL MODEL OF CLOUDS AND METHOD OF SOLUTION

In this work we made use of a modified fractal model of marine stratocumulus clouds *Sc* described in detail in Refs. 1, 6, and 7. Instead of cascade processes, the spectral methods of simulating random processes (fields)[8] are used to generate numerical realizations of the distribution of optical depth. Input parameters to the spectral model are the mean $\langle\tau\rangle$, variance D_τ, and the exponent β of the power-law energy spectrum of the optical depth simulated as a random process with 1D lognormal distribution and a power-law spectrum. A continuous realization of this process is divided into $N_x = 2^{nx}$ pixels with equal horizontal dimensions $\delta x = 0.05$ km. Each pixel is assigned to have the optical depth τ_i, $i = 1, \ldots, N_x$, as a value of the random process at the point corresponding to the left-hand side of the pixel. Then the pixel extinction coefficient is calculated as $\sigma_i = \tau_i / h$, where h is the cloud geometrical depth. In the calculations we used $\langle\tau\rangle = 13$, $D_\tau = 29$, $\beta = 5/3$ and $h = 0.3$ km, which are typical for marine *Sc*.[6,7] The calculations made for the cascade model[1,6,7] with $\delta x = 0.0125$ km and spectral model from Ref. 8 with $\delta x = 0.01$ km are specially underlined in the text.

Numerical simulation of the solar radiation interaction with inhomogeneous *Sc* clouds is performed with the scattering phase function of C_1 cloud,[9] calculated for the wavelength of 0.69 μm by the Mie theory. We assume that there is no absorption by liquid water in the visible spectral range and the single scattering albedo $\omega_0 = 1.0$. The surface albedo is equal to zero, what roughly corresponds to the albedo of the ocean. The number of pixels is $N_x = 2^{12} = 4096$ and, given $\delta x = 0.05$ km, the length of the cloud realization is 204.8 km. Solar incidence is defined by the zenith and azimuth angles, Θ_0 and φ_0. The latter is measured from *OX*-axis and is set to be zero throughout the computation.

0235-6880/99/03 180-07 $02.00

The equation of radiative transfer is solved using the Monte Carlo method and periodic boundary conditions. Using direct simulation, we have calculated the albedo and the reflectance (into different solid angles) for each pixel, as well as the intensity of radiation reflected toward zenith, which we will further call the zenith radiance. The relative computation error does not exceed 1%.

3. GEOMETRIC AVERAGING

We assume that a unit solar flux is incident on the top of the atmosphere (TOA). The reflectance $F(x, H_t, \Theta)$ into different cones of angular width Θ is defined by the formula

$$F(x, H_t, \Theta) = \int_0^{2\pi} d\varphi \int_0^{\Theta} \cos\vartheta\, I(x, 0, H_t, \vartheta, \varphi) \sin\vartheta\, d\vartheta\,, \quad (1)$$

where $I(x, 0, H_t, \vartheta, \varphi)$ is the intensity of the reflected radiation, H_t is the cloud top height, ϑ and φ are the zenith and azimuth angles, respectively. By definition, the cloud albedo $R(x) = F(x, H_t, 90°)$.

The reflectance $F(x, H_t, \Theta)$ is formed owing to the radiation, which, before reaching the detector, is scattered in some effective volume V_e (Fig. 1). This volume contains a set of points $\mathbf{r}_0 = (x_0, y_0, z_0)$ falling within the detector's FOV and satisfying the inequality $\sqrt{(x_0 - x)^2 + y_0^2 + (z_0 - H_t)^2} \le R_e$. Here $R_e \le h/\cos\Theta$ is an effective radius depending on the detector's spatial position and the FOV, solar zenith angle, as well as optical properties and depth of a cloud $h = H_t - H_b$, where H_b is the cloud base height. It follows from simple physical considerations that, when h = const and the cloud extinction coefficient σ increases, the effective radius decreases, and in the limit at $\sigma \to \infty$ and $R_e \to 0$ the detector does not integrate (average) over space. For convenience, the effect associated with averaging of radiation over finite detector's FOV will be referred to as the geometric averaging.

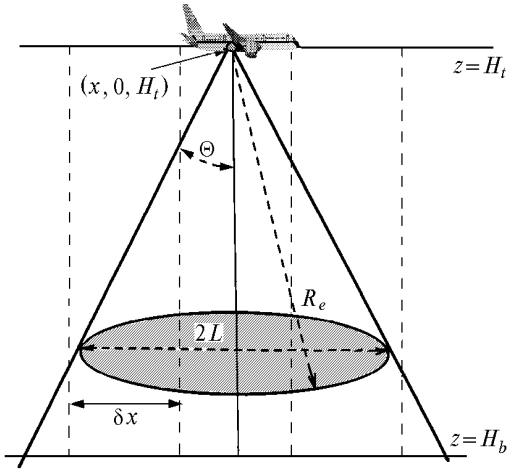

FIG. 1. Schematic of the geometric averaging effect caused by the finite detector's FOV.

This effect depends on two scaling parameters: the horizontal size of a pixel δx and the distance $L = R_e \sin\Theta \le h \tan\Theta$. At $L \le \delta x/2$, the detector receives the radiation scattered within a single pixel, so the finiteness of the detector's FOV has no smoothing (averaging) effect on the random process $F(x, H_t, \Theta)$. At $L \gg \delta x$, many pixels fall within the detector's FOV, so the geometric averaging smoothes out the random process $F(x, H_t, \Theta)$ and makes it weakly sensitive to cloud inhomogeneities on the spatial scales $r \sim \delta x$; in other words, $F(x, H_t, \Theta)$ in this case weakly depends on small-scale cloud inhomogeneities and thus is a smoother function than at $L \le \delta x/2$.

Barker[3] has studied the geometric averaging effect on the spatial spectra of albedo calculated for the detector located at some height above the cloud top. He has claimed that the geometric averaging effect does not explain the presence of the scale break in the spatial spectrum of albedo and its absence for the reflectance at 5°, $F(x, H_t, 5°)$, in the case when the reflected radiation field is calculated strictly at the cloud top height. Barker argues that the distribution of distances between the points of photon entry and exit is practically identical for albedo and $F(x, H_t, 5°)$. This argument seems to be unconvincing, for it remains unclear how the identity of the distributions of distances between the points of photon entry and exit is related to the geometric averaging effect. Moreover, the author does not consider the geometric averaging in the case when the detector is located at the cloud top/bottom boundary or inside the cloud, thus implicitly assuming that the geometric averaging can be neglected in this case. Below we will show that the geometric averaging effect plays central role in physical interpretation of spatial spectra of the radiative field, regardless of whether the detector is located beyond, at the boundaries, or inside a cloud.

The segment of realization of the ratio $F(x, H_t, \Theta)/\overline{F(H_t, \Theta)}$ calculated at the cloud top boundary for Θ = 10, 30, 60° and two solar zenith angles Θ_0 = 0 and 60° is a direct illustration of the geometric averaging effect (Fig. 2). From here on the overbar denotes the average over realization of cloud optical depth. For h = 0.3 km and Θ = 60°, the maximum value $L_{max} = h \tan 60° \sim 0.5$ km, and the number of pixels contributing to $F(x, H_t, 60°)$ can reach 20. Because of averaging over so large number of pixels, the ratio $F(x, H_t, 60°)/\overline{F(H_t, 60°)}$ is a much smoother function than $F(x, H_t, 10°)/\overline{F(H_t, 10°)}$, when no more than two pixels fall within the detector's FOV.

The spatial spectra of $F(x, H_t, \Theta)$ are presented in Fig. 3. If in each individual measurement the instrument receives (averages) the radiation from ~ 10–20 pixels (Θ = 30–90°), then the small-scale features of the radiative field are smoothed out, and

the spatial spectrum of $F(x, H_t, \Theta)$ has a break at some characteristic scale η. Averaging over two pixels is insufficient to smooth $F(x, H_t, 10°)$, and, for this reason, the scale break is not observed. The latter is in accord with the results by Barker,[3] who found no scale break in the spectrum of $F(x, H_t, 5°)$.

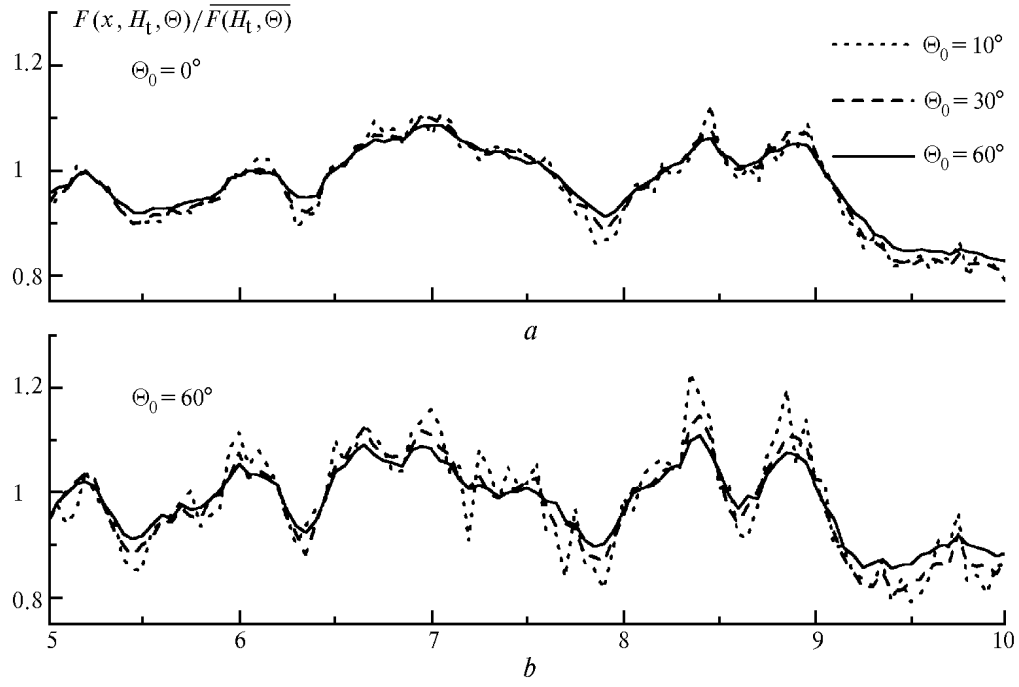

FIG 2. A fragment of realization of the $F(x, H_t, \Theta)/\overline{F(H_t, \Theta)}$ *ratio for two solar zenith angles:* $\Theta_0 = 0$ *(a) and* 60° *(b). The wider the detector's FOV, the smoother the behavior of the ratio.*

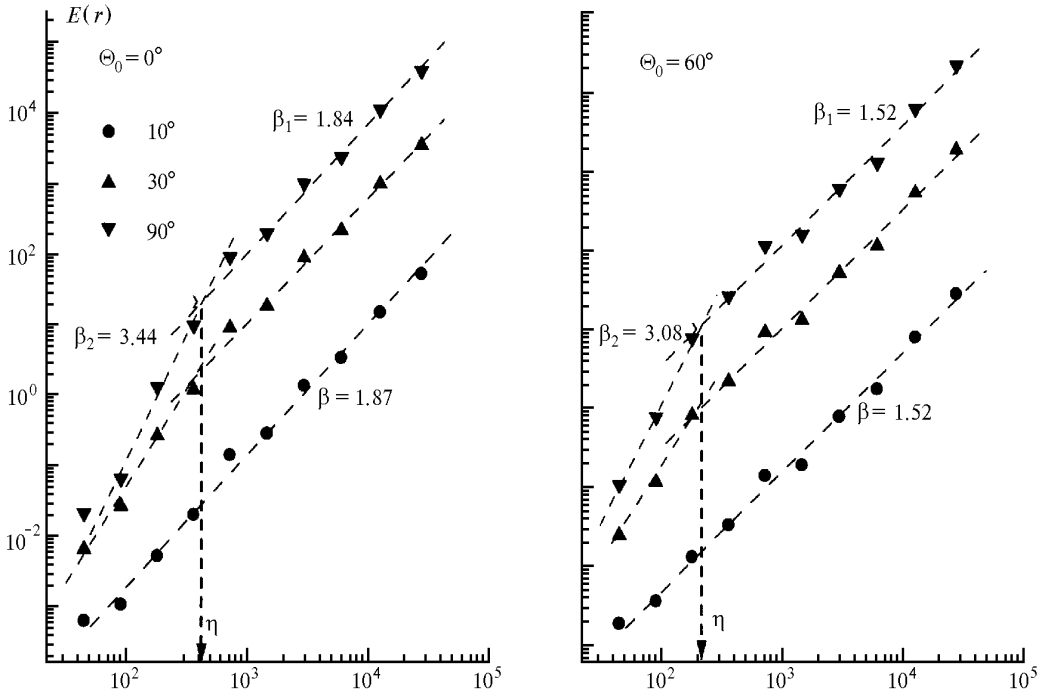

FIG. 3. Spatial spectra of the reflectance into cones of different angular widths $\Theta = 10, 30, 90°$. *For* 10° *reflectance, the geometric averaging has a little smoothing effect on the radiation field and causes no scale break. The larger* Θ_0, *the smaller the scale* η.

As solar zenith angle increases from 0 to 60°, the characteristic scale η decreases by approximately a factor of two (Fig. 3). Horizontal radiative flux E, excited by horizontal cloud inhomogeneity, cannot cause such a decrease in the scale η. Because of a strong forward peak of the cloud scattering phase function, at oblique sun angles the radiation energy can be exchanged between, on the average, wider separated

pixels; therefore, with growing Θ_0, the correlation radius of E will rather increase (see Fig. 4*a*). A possible explanation for the η decrease might be the fact that at $\Theta_0 = 0$ solar radiation penetrates deeper into the cloud; therefore, the detector averages over a larger number of pixels, and the effective radius R_e increases. To validate this explanation, the vertical profiles were calculated for the mean (over optical depth realization) upward flux inside ($0 \le z \le H_t - H_b$) inhomogeneous clouds (Fig. 4*b*). It is seen that at $z \le 0.24$ km the mean upward flux decreases with increasing Θ_0. Thus, as Θ_0 increases from 0 to 60°, the effective radius does decrease, and geometric averaging successfully explains the decrease in the scale η.

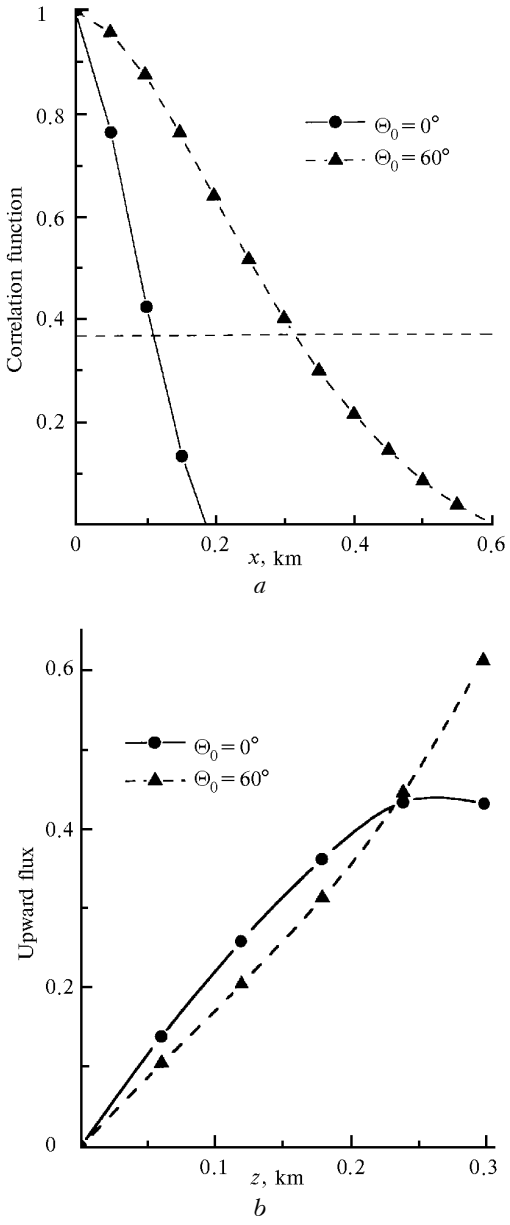

FIG. 4. Autocorrelation functions of horizontal transport (a) and mean upward flux for two solar zenith angles: $\Theta_0 = 0$ *and* 60° *(b).*

The absence of the scale break for 5° and 10° reflectance allows us to assume that there is such a value of Θ_* that $F(x, H_t, \Theta)$ has (has no) the scale break at $\Theta > \Theta_*$ ($\Theta < \Theta_*$). If this speculation is correct, then the spatial spectrum of the zenith radiance $I(x, 0, H_t, 0, 0)$ must not have a scale break. The random functions $I(x, 0, H_t, 0, 0)$ were calculated for the spectral model (SM) with the pixel size $\delta x = 50$ m and for the cascade model (CM) with $\delta x = 12.5$ m. The spatial spectra of zenith radiance have no scale break (Fig. 5), what confirms our assumptions.

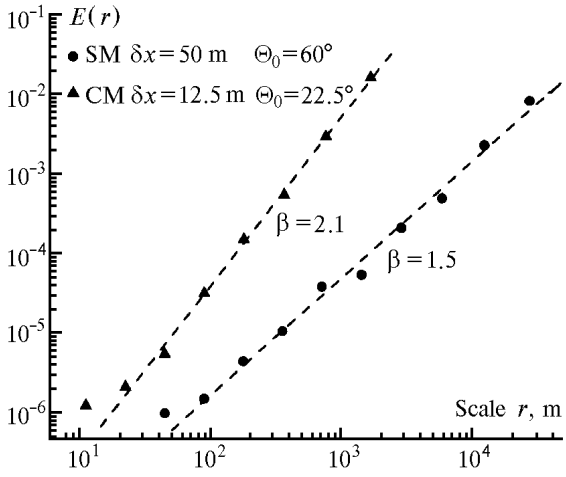

FIG. 5. Spatial spectra of zenith radiance for the spectral (SM) and cascade (CM) models of stratocumulus clouds. Because of the absence of geometric averaging, there is no scale break.

Thus, our results support the important role of the geometric averaging in smoothing the radiative field and forming the scale break: if geometric averaging is small or completely absent, then the spatial spectrum of the measured radiation field has no scale break.

4. RADIATIVE SMOOTHING AND THE SCALE BREAK

The narrower the detector's FOV, the weaker the geometric averaging effect; that is why the $F(x, H_t, \Theta)$ spectrum for $\Theta \le 10°$ (Fig. 3) and, in particular, the spectrum of zenith radiance (Fig. 5), do not exhibit any scale break. The latter does not agree with the findings of Marshak et al.[4] and Davis et al.[5] Using a cascade model of stratocumulus clouds and the Monte Carlo method, they have found that the *structure functions* of the zenith radiance have the scale break. Referring to Wiener–Khinchin theorem for homogeneous and isotropic fields, they assert that the spatial spectrum of zenith radiance ought to have the scale break as well. A reader will find in these papers no evidences that the scale break *of the spatial spectrum* of zenith radiance has been obtained by numerical simulation. Nevertheless, the authors claim that they explained the Landsat scale break: "The mechanism of this scale break is now clear: horizontal

radiative transport smoothes out the small-scale features of the underlying extinction field.B[4] For this effect of horizontal radiation fluxes, they use the term "radiative smoothing.B

The physical mechanism of the radiative smoothing has not been clearly defined and has been formulated only intuitively. The authors restrict themselves to only visual comparison of realizations of the zenith radiance calculated by Monte Carlo (MC) method and by the independent pixel approximation (IPA). Obviously, such a comparison will give no answer to the key (for their explanation) question: how often and why does the horizontal radiative flux smooth out the small-scale features of the radiation field. This question is not unreasonable, because, as known, the horizontal radiative transport can both decrease and, on the contrary, increase the amplitude of albedo fluctuations, so that albedos far in excess of unity may be sampled.[4,10] The IPA and MC albedos $R_{\mathrm{IPA}}(x)$ and $R_{\mathrm{MC}}(x)$ are shown in Fig. 6. A visual comparison shows that $R_{\mathrm{MC}}(x)$ is not a smoother function than $R_{\mathrm{IPA}}(x)$; thus, the horizontal flux does not always smooth the radiative field. However, $R_{\mathrm{MC}}(x)$ has the scale break, whereas $R_{\mathrm{IPA}}(x)$ has no (Fig. 3). Recall that there is no geometric averaging in IPA.

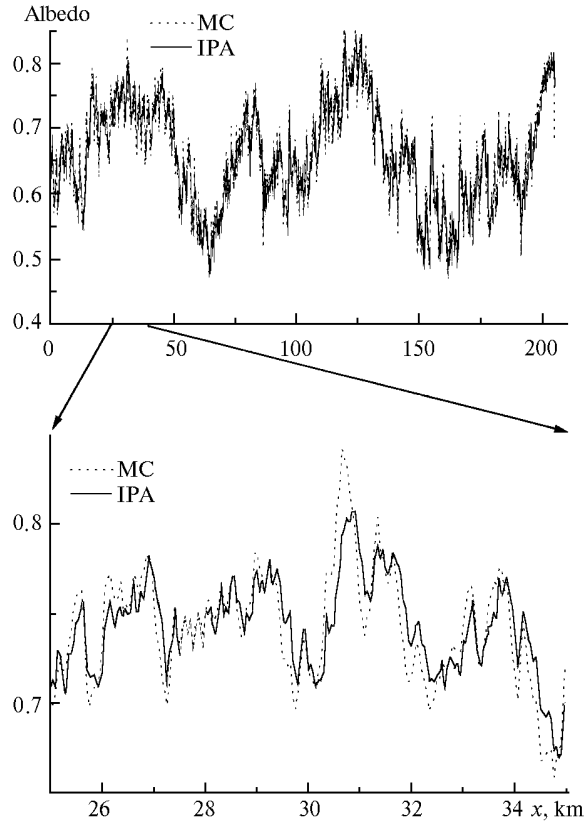

FIG. 6. The IPA and MC albedos $R_{\mathrm{IPA}}(x)$ and $R_{\mathrm{MC}}(x)$ as functions of the distance x (km) for solar zenith angle $\Theta_0 = 60°$; $R_{\mathrm{MC}}(x)$ does not appear to be a smoother function than $R_{\mathrm{IPA}}(x)$.

For zenith radiance there is no integration over the detector's FOV and, hence, no geometric averaging; whereas for albedo this effect is maximum. So, it is unclear why do the structure functions of zenith radiance and albedo have the scale breaks at the same characteristic scale (Ref. 4, Fig. 12). The authors do not explain this fact.

According to Refs. 4 and 5, the characteristic scale η is proportional to $\sqrt{\overline{\rho^2}}$, where $\overline{\rho^2}$ is the second moment of the distribution of distances between the points of photon entry and exit. In the diffuse approximation, $\sqrt{\overline{\rho^2}}$ is related to cloud parameters by the formula

$$\sqrt{\overline{\rho^2}} \approx \begin{cases} h[(1-g)\tau]^{-1/2} & \text{for albedo,} \\ h & \text{for transmittance,} \end{cases} \qquad (2)$$

where h is the cloud geometric thickness, g is the asymmetry factor, and τ is the optical depth. For inhomogeneous clouds, we propose to use the mean (over realization) optical depth $\bar{\tau}$ instead of τ. From Eq. (2) we conclude that $\sqrt{\overline{\rho^2}}$ depends on the standard parameters h, g, and τ, determining the radiative transfer in inhomogeneous clouds, and is independent of horizontal variability of the cloud optical properties. Horizontal radiative fluxes, which supposedly define the scale η, depend primarily on the horizontal gradient of optical depth. With a variation of the horizontal gradient of $\tau(x)$ the scale η changes, while $\sqrt{\overline{\rho^2}}$ remains the same. For this reason, no one-to-one relationship exists between η and $\sqrt{\overline{\rho^2}}$, and, generally speaking, $\sqrt{\overline{\rho^2}}$ cannot determine η. This is an additional argument supporting the statement that the classic one-dimensional radiative transfer theory fails to explain physically and to quantify accurately the radiative effects caused by horizontal variability of the optical properties of real clouds.

Further, according to Eq. (2), the value of $\sqrt{\overline{\rho^2}}$ does not change under linear transformation $h' \to \alpha h$ and $\tau'(x) \to \alpha^2 \tau(x)$, and, hence, the scale break should occur at one and the same scale η. To validate this statement, the realizations of $F(x, H_{\mathrm{t}}, 10°)$, $F(x, H_{\mathrm{t}}, 30°)$, and albedo were calculated at the scale parameter $\alpha = 2.3$. The corresponding spatial spectra are presented in Fig. 7. The most important result is that, in contrast to the case of $\alpha = 1$, at $\alpha = 2.3$ both $F(x, H_{\mathrm{t}}, 10°)$ and $F(x, H_{\mathrm{t}}, 30°)$ have no scale break (see Fig. 3*a*). Hence, under such linear transformation, the spatial spectrum of $F(x, H_{\mathrm{t}}, 30°)$ either can ($\alpha = 1$) or cannot have ($\alpha = 2.3$) the scale break, which means that there is no conservation of the scale η. As to the spatial spectrum of albedo, with an increase of parameter α from 1 to 3, the scale η does not remain constant but increases from ~ 0.4 to ~ 0.6 km.

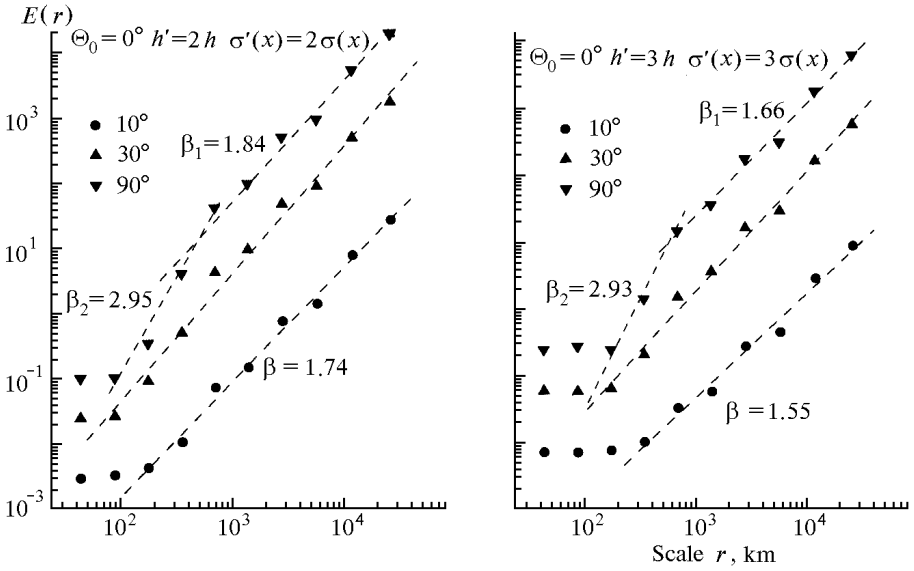

FIG. 7. Spatial spectra of the reflectance at $\Theta_0 = 0°$ *and optical depths* $\tau' = \alpha^2\tau(x)$ *with* $\alpha = 2$ *(a) and* $\alpha = 3$ *(b); there is no scale break in the reflectance at* 30°.

The behavior of the spatial spectra presented in Figs. 3 and 7 could be explained by the geometric averaging effect. Maybe, with an increase in optical depth, the effective radius R_e for the reflectance $F(x, H_t, 30°)$ decreases; therefore, the detector averages over a smaller number of pixels, and there is no scale break at $\alpha = 2.3$. For albedo, an increase in the cloud geometric thickness h possibly causes some increase of R_e; hence, the detector averages over a larger number of pixels, so the scale η increases. We use here the words "maybeB and "possiblyB in order to emphasize a dearth of knowledge about the dependence of the effective radius on the detector's FOV, geometric and optical properties of clouds, solar zenith angle, and on the surface albedo. The geometric averaging effect has a great potential for improving physical interpretations of field measurements; therefore, it deserves a further study.

Our findings clearly show that the explanation of the scale break based on the radiative smoothing as well as the proposed interrelation between η and $\sqrt{\overline{\rho^2}}$ are physically incorrect. Moreover, they even cast doubts on the existence of the radiative smoothing effect itself.

For scales less than 0.1–0.2 km, the spatial spectra of albedo and $F(x, H_t, \Theta)$ look like spectra of white noise. Barker[3] first noted this feature and explained it as follows: "The white noise arises from the sensor responding to signals from many regions of the cloud that are uncorrelated with each other.B However, his argument fails to explain the absence of the white noise at $\alpha = 1$ (Fig. 3*a*) and its presence at large mean optical depth (Fig. 6). We calculated the cloud radiative properties under discussion by the Monte Carlo method with relative computation error less than 1%. The larger the cloud optical depth, the greater the reflectance $F(x, H_t, \Theta)$ and albedo, and, hence, the higher the absolute errors of computation. In optically thick clouds, $F(x, H_t, \Theta)$ and albedo weakly depend on the optical depth and increase insignificantly in response to its large increments. This implies that at $\alpha = 2.3$, the small-scale (0.1–0.2 km) fluctuations of $F(x, H_t, \Theta)$ and albedo are comparable to the absolute error of computation; and because the latter is an uncorrelated random process, the spectrum of white noise is observable on these spatial scales.

5. CONCLUSION

The influence of geometric averaging on the spatial spectra of reflected radiation has been studied using numerical simulation technique. Our results confirm the widely accepted viewpoint that the geometric averaging effect on the reflectance spectra must be taken into account independently of whether the detector is located beyond, at the boundaries, or inside the cloud.

If the detector receives radiation from one or two pixels, then it does not smooth out the spatial fluctuations of the radiation field so they are well described by the power-law spectrum without any scale break. Averaging over 10–20 pixels is sufficient to make the albedo and the reflectance smoother functions and to give rise to the scale break in their spatial spectra. This result clearly shows that multiple scattering and/or horizontal radiative transport, independent of the detector's FOV, cannot smooth out the small-scale variability of the radiative field.

Because of the horizontal radiative transport, the amplitude of albedo fluctuations may increase, and the sampling values of albedo can exceed unity.[4,10] The MC albedo does not appear to be a smoother function

than its IPA counterpart. These results, as well as the absence of the scale break for 10° (at larger optical depth) and 30° reflectance and zenith radiance, prove the inability of horizontal radiative fluxes to smooth out the radiative field and cause the scale break in its spectrum. Hence, our results do not confirm the radiative smoothing explanation of the scale break.[4,5] If the detector is installed onboard an aircraft, the presence or absence of the scale break in the spatial spectrum of the reflected radiation can be explained by the geometric averaging effect.

Evidently, the geometrical averaging effect fails to explain the scale break in spectra of reflected radiation, inferred from high spatial resolution (~30 m) (and, hence, narrow FOV) Landsat data. More attention should be paid to the statistical explanation developed in Ref. 2. Probably, the causes of the scale break are the insufficient amount of samples and/or the statistical inhomogeneity of real cloud systems.

REFERENCES

1. R.F. Cahalan and J.B. Snider, Remote Sens. Environ. **28**, 95–107 (1989).
2. S. Lovejoy, D. Schertzer, P. Silas, Y. Tessier, and D. Lavalle, Ann. Geophys. **11**, 119–127 (1993).
3. H.W. Barker, Remote Sens. Environ. **54**, 113–120 (1995).
4. A. Marshak, A. Davis, W. Wiscombe, and R. Cahalan, J. Geophys. Res. **100**, No. D12, 26247–26261 (1995).
5. A. Davis, A. Marshak, R. Cahalan, and W. Wiscombe, J. Atmos. Sci. **54**, No. 2, 241–260 (1997).
6. R.F. Cahalan, W. Ridgway, W.J. Wiscombe, T.L. Bell, and J.B. Snider, J. Atmos. Sci. **51**, No. 16, 2434–2455 (1994).
7. R.F. Cahalan, W. Ridgway, W.J. Wiscombe, S. Gollmer, and Harshvardhan, J. Atmos. Sci. **51**, 3776–3790 (1994).
8. S.M. Prigarin and G.A. Titov, Atmos. Oceanic Opt. **9**, No. 7, 629–635 (1996).
9. D. Deirmendjian *Electromagnetic Scattering on Spherical Polydispersions* (American Elsevier Publishing Company, New York, 1969), 298 pp.
10. G.A. Titov, Atmos. Oceanic Opt. **9**, No. 1, 1–7 (1996).